AGU PUBLICATIONS

JGR

Journal of Geophysical Research: Space Physics

RESEARCH ARTICLE
10.1002/2015JA021781

Electron trapping and acceleration by kinetic Alfven waves in the inner magnetosphere

A. V. Artemyev[1,2], R. Rankin[3], and M. Blanco[3]

[1]Space Research Institute, RAS, Moscow, Russia, [2]Now at Institute of Geophysics and Planetary Physics, University of California, Los Angeles, California, USA, [3]Department of Physics, University of Alberta, Edmonton, Alberta, Canada

Key Points:
- Kinetic Alfven waves in the equatorial inner magnetosphere can trap 100 eV electrons
- Tapped electrons are accelerated up to energies of several keV
- Trapping acceleration results in a significant decrease of the electron equatorial pitch angle

Correspondence to:
A. V. Artemyev,
Ante0226@gmail.com

Citation:
Artemyev, A. V., R. Rankin, and M. Blanco (2015), Electron trapping and acceleration by kinetic Alfven waves in the inner magnetosphere, *J. Geophys. Res. Space Physics*, *120*, 10,305–10,316, doi:10.1002/2015JA021781.

Received 6 AUG 2015
Accepted 12 NOV 2015
Accepted article online 14 NOV 2015
Published online 8 DEC 2015

Abstract In this paper we study the interaction of kinetic Alfven waves generated near the equatorial plane of the magnetosphere with electrons having initial energies up to ~100 eV. Wave-particle interactions are investigated using a theoretical model of trapping into an effective potential generated by the wave parallel electric field and the mirror force acting along geomagnetic field lines. It is demonstrated that waves with an effective potential amplitude on the order of ~100–400 V and with perpendicular wavelengths on the order of the ion gyroradius can trap and efficiently accelerate electrons up to energies of several keV. Trapping acceleration corresponds to conservation of the electron magnetic moment and, thus, results in a significant decrease of the electron equatorial pitch angle with time. Analytical and numerical estimates of the maximum energy and probability of trapping are presented, and the application of the proposed model is discussed.

1. Introduction

Hot (few keVs) electron populations in Earth's inner magnetosphere play an important role in the generation of whistler waves [e.g., *Li et al.*, 2010; *Fu et al.*, 2014; *Mourenas et al.*, 2015, and references therein] and in scattering electrons into the atmosphere to produce diffusive aurora [e.g., *Arnoldy*, 1974; *Akasofu*, 1974]. Besides convection and (or) substorm injections of hot magnetotail electrons into the inner magnetosphere [e.g., *Gabrielse et al.*, 2012; *Ganushkina et al.*, 2013, and references therein], local acceleration of cold ionospheric electrons represents a promising scenario for formation of hot electron populations. Effective acceleration of cold magnetized electrons is usually provided by wave-particle resonant interactions. In the inner equatorial magnetosphere sub-keV electrons (~100 eV) can resonate with electron cyclotron harmonics [e.g., *Horne et al.*, 2000], upper band chorus waves [e.g., *Ni et al.*, 2011b], very oblique low band chorus waves [*Artemyev et al.*, 2015], kinetic Alfven waves (KAWs) [e.g., *Hasegawa*, 1976; *Wygant et al.*, 2002], and broad low-frequency electrostatic noise that consists of a mixture of electron holes and double layers [*Mozer et al.*, 2015, and references therein]. Excitation and amplification of wave emissions is also closely related to injections from the magnetotail [*Angelopoulos et al.*, 2002; *Ni et al.*, 2012; *Mozer et al.*, 2014; *Malaspina et al.*, 2015; *Ergun et al.*, 2015]. Scattering of sub-keV electrons by upper band chorus and electron cyclotron waves mainly results in precipitation, while parallel electric fields of very oblique low band chorus waves, KAWs, and electrostatic noise, can effectively accelerate electrons along magnetic field lines.

Phase velocities of very oblique low band chorus waves are comparable with thermal electron velocities for electron energies between 100 and 1000 eV, and thus, Landau resonance interaction is possible [*Artemyev et al.*, 2012]. In contrast, the phase velocity of KAWs is too low at the equatorial region around L shells 6–9 to allow these waves undergo Landau resonance with ~100 eV electrons (situation is different for aurora region where high amplitude of Alfven velocity becomes comparable with thermal electron energy running the Landau resonance interaction) [see, e.g., *Chaston et al.*, 2000, 2002]. However, the amplitude of the wave potential for KAWs is large enough to effectively expand the range of resonance velocities. Although a full understanding of the interaction between KAWs and electrons remains unclear, but parallel electric fields are known to play an important role [*Kletzing et al.*, 2003; *Damiano and Wright*, 2005; *Chaston et al.*, 2008, 2012; *Watt et al.*, 2004, 2005, 2006]. The magnitude of parallel electric fields in KAWs can be many times larger in the plasma sheet than above the ionosphere [*Watt and Rankin*, 2009] and can drive wave-particle interactions via at least three mechanisms: diffusive-like electron heating [e.g., *Hasegawa and Mima*, 1978; *Potapenko et al.*, 2000; *Tikhonchuk and Rankin*, 2002; *Lysak and Song*, 2003], acceleration due to reflection of electrons from the wave potential wall [*Kletzing*, 1994], and possible electron trapping. The later mechanism was proposed by

Hasegawa and Mima [1976] for soliton-like KAW trapping of electrons into a potential well formed by parallel electric fields. This classical trapping effect is significantly modified in the case of inhomogeneous plasma [*Laval and Pellat*, 1970; *Karpman and Shklyar*, 1972] and magnetic field gradients [*Nunn*, 1971; *Karpman et al.*, 1974].

Wave propagation along dipole magnetic field lines away from the equatorial plane has two effects on electrons: (1) the competition of the wave parallel electric field and mirror force can generate an effective potential well for trapped electrons, and (2) trapped particles moving with the wave velocity along the spatially growing magnetic field are accelerated due to conservation of the first adiabatic invariant (magnetic moment). This mechanism of acceleration works well for very oblique whistler waves [*Artemyev et al.*, 2012] and for electrostatic double layers [*Artemyev et al.*, 2014]. Recent numerical modeling [*Watt and Rankin*, 2009, 2010] suggests that a similar mechanism can be realized in a system with KAWs. Moreover, modern spacecraft observations reveal an abundance of such waves in the equatorial inner magnetosphere [*Chaston et al.*, 2014; *Ergun et al.*, 2015] where they are correlated with the presence of low-frequency electrostatic noise [*Mozer et al.*, 2013, 2015; *Malaspina et al.*, 2015]. Thus, detailed parametric investigation of sub-keV electron trapping and acceleration by KAWs represents an interesting and important problem.

In this paper we generalize the approach proposed by *Artemyev et al.* [2014] to account for electron interactions with KAWs having a finite transverse scale on the order of the ion gyroradius. We propose a new theoretical model describing electron trapping by KAWs and estimate the maximum energy that can be gained by trapped electrons.

2. Electron Trapping and Acceleration

Superthermal electrons can efficiently interact with intense KAW having a pronounced parallel electric field component. Such fields do not significantly perturb the electron gyromotion, and thus, the first adiabatic invariant (magnetic moment) is conserved. In this case, Landau resonance $k_{\|}v_{\|} = \omega$ between waves with frequency ω and electrons moving with the parallel velocity $v_{\|}$ should be considered. Resonance implies that the wave parallel phase velocity $\omega/k_{\|} \sim v_A$ is approximately the same magnitude as the electron thermal velocity (v_A is the Alfven velocity). Around L shell ~9 the Alfven speed v_A amplitude is generally less than about 2000 km/s, while electron thermal velocities (for energy 50–500 eV) are about 4000–13,000 km/s. Therefore, the resonant condition $k_{\|}v_{\|} = \omega$ cannot be easily satisfied. However, the presence of a parallel electric field provides an efficient widening of the resonance region [e.g., *Karney*, 1978], making resonance more favorable: $v_{\|} \in [\omega/k_{\|} \pm \sqrt{eE_{\|}/m_e k_{\|}}]$ with m_e and e the electron mass and charge, respectively. For scalar potential amplitudes $\Phi_0 \sim E_{\|}/k_{\|} \sim$100–400 V the resonant condition can be satisfied easily for electrons with energies up to 550 eV. Electrons in this energy range are consequently trapped by waves into Landau resonance and are able to reach higher latitudes than they normally do. As they move along field lines conserving their magnetic moment they are efficiently accelerated (see examples of such acceleration mechanism in *Artemyev et al.* [2012, 2014]). The efficiency of electron trapping and acceleration by parallel electric fields of KAWs during this interaction is estimated below.

In our analysis the effects of transverse components of the wave electric field are neglected (see section 3) and only parallel electron motion is considered. The wave parallel electric field is described by an effective scalar potential Φ that includes contributions from the electric scalar potential and the parallel component of the magnetic vector potential (see Appendix A). The amplitude of the effective potential is Φ_0, while the wave dispersion relation provides the function $k_{\|}(z)$, where z is the field-aligned coordinate (see equation (A1)). The corresponding wave phase ψ is

$$\psi = \int^{z} k_{\|}(z')\mathrm{d}z' - \omega t + \mathrm{const.} \tag{1}$$

The shape of the wave packet shown in Figure 1 includes variations over a few wave periods (in agreement with numerical models) [e.g., *Watt and Rankin*, 2009].

2.1. Equations of Motion

The geomagnetic topology characteristic of the inner magnetosphere will be considered to be a curvature-free dipole magnetic field $B(\lambda) = B_{eq}b(\lambda)$ [*Bell*, 1984] with a plasma density defined by $n_e(\lambda) = n_{eq}\cos^{\ell}\lambda$ where index $\ell = -5$ is taken from the empirical model presented by *Denton et al.* [2006]

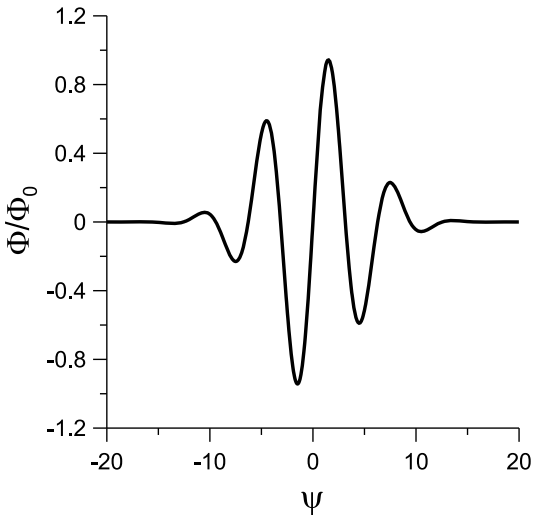

Figure 1. The assumed shape of the kinetic Alfven wave packet. The effective scalar potential is shown.

for L shell ~6–7. The relation between the field-aligned coordinate and magnetic latitude is given by $dz = R_0\sqrt{1+3\sin^2\lambda}\cos\lambda$ and $R_0 = R_E L$, while the equatorial value of the plasma density n_{eq} is given by the *Sheeley et al.* [2001] model. The main deviation of magnetic field configuration from the dipole field at $L \sim 6$–9 (the L shell range considered in this study) corresponds to the near-equatorial region where currents of hot injected ions can significantly deform the magnetic field lines [see, e.g., *Tsyganenko et al.*, 2003]. We explain a possible role of such magnetic field reconfiguration for KAW interaction with electrons in section 3.

We introduce the dimensionless spatial coordinate $s = z/R_0$ and normalized time coordinate $t \to tv_{A,eq}/R_0$, where $v_{A,eq}$ is the equatorial Alfven speed. The corresponding Hamiltonian of electrons includes three terms: the electron kinetic energy corresponding to the motion along magnetic field lines $m_e v^2/2$ (where $v = \dot{s}$), the electron kinetic energy corresponding to the gyrorotation $\mu B(s)$ (where μ is the electron magnetic moment), and the potential energy $\sim \Phi$ (see gyroaveraged equations of motion in *Northrop* [1963]). The dimensionless form of this Hamiltonian can be written as

$$H = \frac{1}{2}v^2 + h\sin^2\alpha_{eq,0}\,b(s) - \phi_0 w(s)F(\psi), \tag{2}$$

where $\alpha_{eq,0}$ is equatorial initial pitch angle and the function $F(\psi) = \Phi/\Phi_0$ is shown in Figure 1. The function $w(s)$ is determined by the dispersion relation (see equation (A5)), $\alpha_{eq,0}$ is the initial equatorial pitch angle, $h \approx 60(E_e/100\,\mathrm{eV})(L/9)^2$, E_e is the initial electron energy, and $\phi_0 \approx 60(\Phi_0/100\mathrm{V})(L/9)^2$. The initial dimensionless particle energy (in absence of waves) is h, while the dimensionless phase (1) is defined by

$$\psi = \chi\left(\int^s K(s')ds' - t\right), \tag{3}$$

where $K(s)$ is given by equation (A2), $\chi \approx 250(2s/T)(L/9)^2$, and T is the wave period (see Appendix A). For all calculations in this paper we use $L = 9$. However, as equation (2) shows, both factors h and ϕ_0 depend on L similarly. Thus, change of the L shell corresponds to multiplication of the initial energy $\sim v^2$ on factor $(9/L)^2$.

The equations of motion corresponding to the Hamiltonian (2) is defined by

$$\begin{aligned}\ddot{s} &= -h\sin^2\alpha_{eq,0}\frac{\partial b}{\partial s} + \phi_0\frac{\partial w}{\partial s}F + \phi_0\chi K w\frac{\partial F}{\partial\psi}\\ &\approx -h\sin^2\alpha_{eq,0}\frac{\partial b}{\partial s} + \phi_0\chi K w\frac{\partial F}{\partial\psi}\\ \dot{\psi} &= \chi\,(K\dot{s} - 1)\end{aligned} \tag{4}$$

where we have taken into account that $\chi \gg 1$. Profiles of functions $b(s)$, $\partial b(s)/\partial s$, $K(s)$, and $w(s)$ are shown in Figure 2. Spacecraft observations in the equatorial magnetotail suggest that KAWs have a significant amplitude of electrostatic field ~10–100 mV/m, while $k_\perp/k_\parallel$ ratio is within the range 10–100 [e.g., *Chaston et al.*, 2012, 2014]. Thus, almost all observed electric field corresponds to the transverse (relative to the background magnetic field) component. Using the KAW dispersion $k_\perp\rho_s \sim 1$ [*Hasegawa*, 1976] with the ion acoustic gyroradius $\rho_s \sim 50$–100 km (for $L \sim 7$–9, hot ion temperature ~1–10 keV, and hot electron temperature 0.1–3 keV) [e.g., *Denton et al.*, 2005], one can estimate the scalar potential amplitude as Φ_0 ~200–400 V. The corresponding parallel electric field is about ~1 mV/m [see, e.g., *Watt and Rankin*, 2012; *Chaston et al.*, 2012]. Thus, through the paper we consider $\Phi_0 \in [100, 400]$ V and $\lambda_\perp = 2\pi/k_\perp \in [150, 650]$ km.

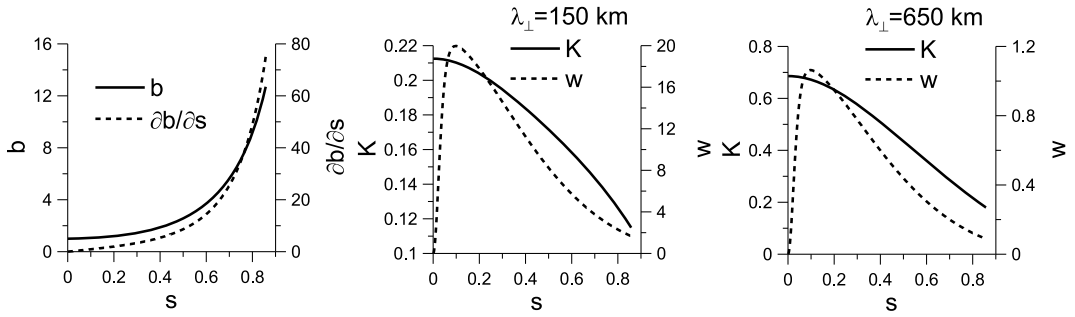

Figure 2. Profiles of functions $b(s)$, $\partial b(s)/\partial s$, $K(s)$, and $w(s)$.

2.2. Test Particle Trajectories

To demonstrate the effect of charged particle trapping and acceleration, we numerically integrate equation (4) for different values of initial electron energy and transverse wavelength $\lambda_\perp$ (see dispersion relation and description of wave model in Appendix A).

Four examples of particle trajectories are presented in Figure 3. Figure 3 (top row) show particle trajectories in the phase plane (s, v) where $v = \dot{s}$. Initially, electrons move along closed trajectories shown by grey small circles. This motion corresponds to electron bounce oscillations between mirror points. On each bounce period, electrons pass through the resonance region with $\dot{\psi} = 0$ (or $v \approx 1/K \pm \sqrt{\phi_0/\chi}$). The corresponding resonant position s_{res} of electrons can be determined from energy conservation in absence of waves: $b(s_{res}) = (2h - K^{-2})/(2h \sin^2 \alpha_{eq,0})$. As $h \sim 60$ for 100 eV electrons, s_{res} is located very close to the mirror point s_{mir} defined by the equation $b(s_{mir}) = 1/\sin^2 \alpha_{eq,0}$. When the wave approaches to s_{res}, electrons can be trapped into the effective potential well. This potential well corresponds to the competition of two forces acting on particles: the wave electric field $\sim \phi_0 \chi KwF'$ compensates the mirror force $\sim h \sin^2 \alpha_{eq,0} b'$. Thus, the mirror force does not decrease the particle parallel velocity, and the trapped particle can move with the wave. Trapping is possible only if this effective potential expands (more precisely, if the area filled by trapped particles in the phase plane increases; see detailed description of the trapping process in *Artemyev et al.* [2010, 2012] and *Neishtadt* [2014]). The wave model described in Appendix A assumes that the wave amplitude (scalar potential) grows within $|\lambda| < 5°$ region near the magnetic equator. At $|\lambda| > 5°$ waves propagate with a constant scalar potential amplitude and all variation of wave amplitude corresponds to wave dispersion (see equation (A5)). Thus, only electrons with large enough equatorial pitch angles (i.e., with small $s_{res} \sim s_{mir}$) can be trapped. For instance, four almost equatorial electrons shown in Figure 3 become trapped and start moving with the wave. The trapped motion (shown by black color) corresponds to electron transport to higher latitudes (larger s) with the resonant velocity $\sim 1/K$. Electron trapped motion corresponds to fast oscillations of wave phase ψ around a resonant value (while $\dot{\psi}$ oscillates around zero). The frequency of these oscillations $\sim \sqrt{\phi_0 \chi}$ is high [e.g., *Artemyev et al.*, 2012], and electrons make a lot of oscillations within the effective potential. In the phase plane $(\psi, \dot{\psi})$ these oscillations can be shown as a quasi-periodic electron motion (see Figure 4).

During the transport of trapped electrons to high latitudes, the electron energy increases as $\sim h \sin^2 \alpha_{eq,0} b(s)$, while the mirror force $\sim h \sin^2 \alpha_{eq,0} b'$ becomes stronger. When electrons reach the position s^* with $h \sin^2 \alpha_{eq,0} b'(s^*) \approx \phi_0 \chi K(s^*) w(s^*) \max F'$ (i.e., the mirror force becomes equal to the wave electric field force), the effective potential vanishes and electrons escape from the resonance [a more accurate definition of the escape coordinate can be found in *Arnold et al.*, 2006]. After escape, electrons start moving along closed trajectories (bounce oscillations) with larger radius (see grey circles in Figure 3 (top row)).

Trapping motion corresponds to two effects: electron acceleration (see Figure 3 (middle row)) and the decrease of electron equatorial pitch angle α_{eq} (see Figure 3 (bottom row)). The later processes are due to electron transport by the wave to high latitudes. Electrons escape in the vicinity of their new mirror points $\sim s^*$ with an energy $H_{fin} \sim h \sin^2 \alpha_{eq,0} b(s^*)$ and velocity $v^* \sim 1/K(s^*)$. Thus, a new equatorial pitch angle can be calculated as $\sin^2 \alpha_{eq} = (1 - \cos^2 \alpha^*)/b(s^*)$ with $\cos \alpha^* = v^*/\sqrt{2H_{fin}} = (h \sin^2 \alpha_{eq,0} K^2(s^*) b(s^*))^{-1/2}$. For large enough s^* we have $\sin^2 \alpha_{eq} \approx 1/b(s^*) \ll \sin \alpha^2_{eq,0} \sim 1$; i.e., we can write the ratio $\sin \alpha_{eq}/\sin \alpha_{eq,0} \approx \sqrt{E_e/H_{fin}}$ where E_e is an initial electron energy. Therefore, electron trapping results in particle acceleration and transport to lower equatorial pitch angle range. Both processes are very effective: electrons shown in Figure 3 gain several hundreds of eV and electron pitch angles decreases down to ~20°–30°.

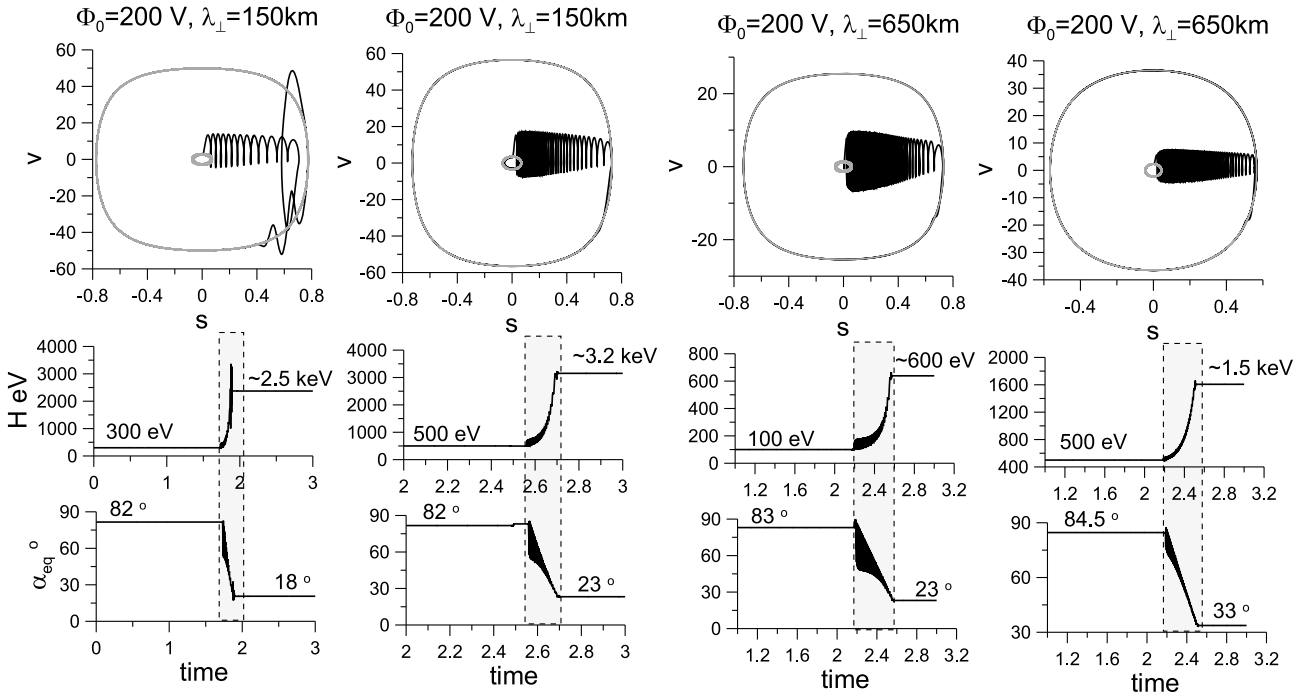

Figure 3. (top row) Four examples of particle trajectories in (s, v) plane. Grey fragments of trajectories show particle bounce oscillations before trapping and after escape from the resonant. (middle and bottom rows) Evolution of particle energy and equatorial pitch angle. Grey color shows the time interval of trapping particle motion.

2.3. Probability of Trapping and Maximum Energies

Figure 3 shows that trapped electrons can be effectively accelerated by the wave. However, the trapping is a probabilistic process [*Neishtadt*, 1999; *Arnold et al.*, 2006]; i.e., only a part of resonant particles can be trapped by waves. The ratio of trapped particles to the whole population of resonant particles can be called a "probability of trapping." This probability can be determined analytically or numerically (see examples in *Shklyar* [1981] and *Artemyev et al.* [2013]). The probability characterizes the efficiency of the acceleration mechanism and, thus, represents the important system parameter. We use the following approach to derive the probability. For a particular value of the initial energy E_e we consider an ensemble of 10^4 particles with a uniform distribution of initial pitch angles α_{eq} and uniform initial distribution along magnetic field lines. We run a single-wave packet (see Figure 2) and numerically integrate particle trajectories. When wave packet reach latitude $\lambda \sim 45°$ we stop numerical integration and collect the final energy spectra. All particles with the final energy $H_{fin} > 1.5E_e$ are assumed to be accelerated due to the trapping mechanism (to exclude the effect of the particle acceleration due to reflection we consider only $H_{fin} > 300$ eV, see section 3 for more details). The probability of trapping is defined as a ratio of trapped (and accelerated) particles to the initial number of particles.

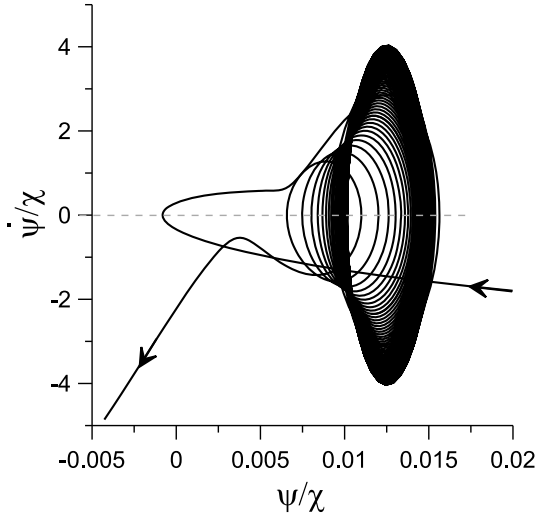

Figure 4. Particle trajectory in the plane $(\psi, \dot{\psi})$. Only fragment of trapped motion is shown.

Figure 5 (left) shows profiles of the probability of trapping as a function of initial electron energy E_e. For $\lambda_\perp = 650$ km the maximum of probability of trapping corresponds to the initial energies $E_e \sim 150–300$ eV. Depending on the wave amplitude Φ_0, 15–40% of resonant particles become trapped and accelerated up to averaged energies

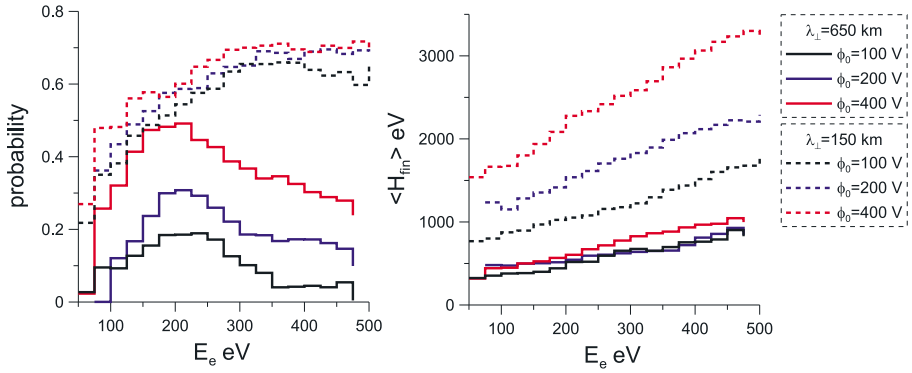

Figure 5. (left) The probability of trapping as a function of the initial energy E_e. (right) The average energies gained by trapped particles.

~500 eV (see Figure 5 (right)). The probability of trapping decreases with the increase of E_e for $E_e > 300$ eV. As an example, the most accelerated particles with $E_e \sim 500$ eV are trapped with a probability < 20%. A low level of probability of trapping for $E_e < 150$ eV is due to our criterion of the final energy $H_{fin} > 300$ eV. Small probability of trapping of energetic electrons with $E_e \sim 500$ eV corresponds to large difference between an electron thermal velocity ($\sim 13,000$ km/s) and resonant velocity (i.e., Alfven speed < 2000 km/s). Thus, only small population of particles can be trapped. The situation changes for waves with $\lambda_\perp = 150$ km. In this case, the wave electric field is significantly stronger (see Appendix A), and the range of resonant velocities becomes wide owing to factor $\sim \sqrt{E_\parallel / k_\parallel}$ [*Karney*, 1978]. As a result, even energetic electrons with $E_e \sim 500$ eV becomes trapped with a probability ~60–70%. These electrons are accelerated up to few keVs on average (see Figure 5 (right)). The expansion of the resonant region in velocity ($\sim \sqrt{E_\parallel / k_\parallel}$) space results also to expansion of the resonant region in the coordinate space (i.e., along magnetic field lines) [e.g., *Artemyev et al.*, 2010]. Thus, even particles located initially at some distance from the equatorial plane can be trapped. These two effects (expansion of the velocity and coordinate resonant ranges) result in the significant increase of the probability of trapping.

KAWs accelerate trapped electrons, transporting them up to the escape position s^* defined by equation $h \sin^2 \alpha_{eq,0} b'(s^*) \approx \phi_0 \chi K(s^*) w(s^*)$. Moreover, to be trapped electrons should have the resonant velocity in the vicinity of the equatorial plane where wave amplitude increases: $\sqrt{2h} \cos \alpha_{eq,0} \approx 1/K(0)$. Thus, we can combine these two equations to derive the single equation for s^*:

$$\frac{1}{K(s^*)w(s^*)} \left.\frac{\partial b}{\partial s}\right|_{s^*} = \frac{2\phi_0 \chi}{2h - K^{-2}(0)} \tag{5}$$

Solution of equation (5) gives s^* as a function of $E_e = h$. Thus, we can substitute this solution to equation for the final energy $H_{fin} \approx h \sin^2 \alpha_{eq,0} b(s^*) = (2h - K^{-2}(0)) b(s^*)/2$ and obtain the maximum energy gained by trapped electrons. Figure 6 presents this maximum energy as a function of initial energy for three values of Φ_0 and two values of transverse wave length $\lambda_\perp$. The maximum energy is about two times larger than the average energy shown in Figure 5 (right).

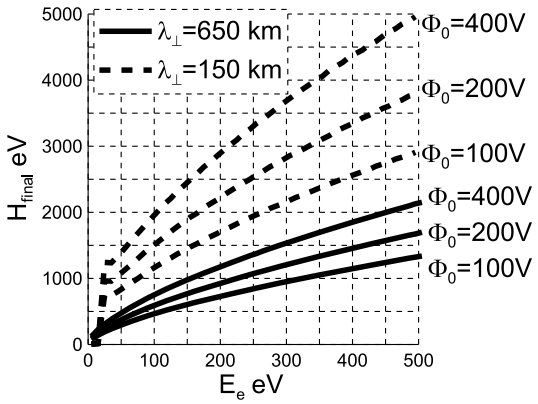

Figure 6. Maximum of energy gained by trapped particles.

3. Discussion

We have focused in this paper on electron acceleration produced by trapping in an effective wave potential, and have not considered Fermi acceleration [*Bryant et al.*, 1991; *Kletzing*, 1994]. It is known that cold electrons with thermal velocity lower than (or about) the wave phase velocity can interact with the moving parallel electric field of a KAW in a manner similar to a ball interacting with a moving wall. Simple reflection of electrons from such a *wall*

results in an energy gain about $\sim 2mv_A^2$. In the case of a large amplitude KAW scalar potential, reflected electrons can gain energy $\sim mv_A\sqrt{e\Phi_0/m}$ (see description of this acceleration mechanism for electron interaction with double layers in *Vasko et al.* [2015]). The maximum energy of reflected electrons is consequently less than 100 eV (for $\Phi_0 < 400$ V). Therefore, Fermi acceleration can be responsible for heating of cold ionospheric electrons (< 10 eV) by KAWs but cannot produce easily a keV population.

One limitation of our analysis is that we have not taken into account the effect of transverse electric field components of KAWs. Although the transverse components are much larger than the parallel one [e.g., *Watt and Rankin*, 2012, and references therein], these components can significantly perturb electron motion only in two cases: provided the cyclotron resonant condition is satisfied or if the effect of finite electron gyroradius ρ_e becomes important. The cyclotron resonance condition is $v_\parallel = (\omega - \Omega_c)/k_\parallel$, where Ω_c is electron cyclotron frequency [*Schulz and Lanzerotti*, 1974]. The corresponding electron energy is significantly larger than a typical hot electron temperature; i.e., this resonance is unavailable for thermal electrons. The second effect of strong electric field gradients (when a spatial scale of electric field becomes comparable with the electron gyroraidus) [see *Balikhin et al.*, 1993] requires $\lambda_\perp \sim \rho_e$. This condition cannot be satisfied for KAW with $\lambda_\perp \sim \rho_s$ where ρ_s is an ion acoustical scale (see Appendix A and *Hasegawa* [1976]). Thus, transverse electric field components can be neglected from consideration as an effective acceleration mechanism.

To simplify analytical estimates and numerical model, we use the dipole approximation for the background magnetic field. However, for nightside magnetosphere at $L \sim 6$–9 the magnetic field configuration can be substantially deformed by currents of hot ions injected from the plasma sheet [*Tsyganenko et al.*, 2003; *Sitnov et al.*, 2008]. Such deformation results in decrease of the equatorial magnetic field B_{eq} and stretching of magnetic field lines. Thus, the equatorial energy of resonant particles $\sim v_{A,eq}^2 \sim B_{eq}^2$ can be significantly decreased. The final energy of accelerated electrons is defined by the position where electrons escape from the resonance at high latitudes. In this region deformations of magnetic field are insignificant [*Tsyganenko et al.*, 2003; *Sitnov et al.*, 2008]. Therefore, for the deformed magnetic field configuration one can expect the trapping of colder electrons, but the acceleration efficiency (the final energies) should be the same as for the dipole magnetic field. The escape position s^* given by equation (5) depends on $K(s)$ function including the variation of the plasma density along magnetic field lines (see equation (A2)). We use the model of the plasma density variation $n_e \sim \cos^{-5}\lambda$ presented by *Denton et al.* [2006]. However, this model is well justified only for $L \leq 7$. The stronger variation of n_e with magnetic latitude λ should result in larger s^* and, thus, leads to the stronger electron acceleration. Quantitative estimates of this effect requires more detailed models of $n_e(\lambda)$.

Our calculations have shown that trapping of sub-keV electrons by KAWs results in an acceleration up to few keV, with a corresponding decrease of the equatorial pitch angle. Thus, trapped and accelerated electrons should form predominantly field aligned distributions or even beams. Subsequent relaxation of these beams should lead to excitation of electrostatic structures (e.g., electron holes and double layers; see modeling in *Génot et al.* [2004] and *Mottez and Génot* [2011]) and very oblique whistler waves [e.g., *Mourenas et al.*, 2015]. This process naturally represents energy cascading from large (ion) scales corresponding to KAWs, to smaller (electron) scales of double layers and whistler waves. Indeed, *Mozer et al.* [2014] and *Malaspina et al.* [2015] show that intensification of electrostatic structures is strongly related to plasma injections bringing into the inner magnetosphere a wide spectrum of KAWs [*Chaston et al.*, 2014; *Ergun et al.*, 2015].

Figure 5 demonstrates that the electron probability of trapping can become very large (close to 80%) in certain cases. This strongly nonlinear regime should cause strong damping of KAWs by the large population of electrons that are trapped and accelerated. However, regular detection of strong KAWs by spacecraft [e.g., *Wygant et al.*, 2002; *Chaston et al.*, 2014] points to a mechanism responsible for wave amplification. One possibility is due to the competition of effects of trapped and transient particles in the system with nonlinear wave-particle interaction [e.g., *Shklyar*, 2011]. Indeed, the acceleration of trapped particles can be compensated by noticeable deceleration of a much larger amount of transient particles scattered by the wave electric field. Particles loosing energy due to interaction with KAW will move ahead of the wave and reflect from the scalar potential with a velocity decrease (see the similar mechanism of particle deceleration due to interaction with electrostatic double layers) [*Vasko et al.*, 2015]. Figure 7 shows an example of transient particle trajectory reflecting from the wave potential with a loss of energy. Particles with different initial energy lose the same energy ~40 eV corresponding to $\sim mv_A\sqrt{e\Phi_0/m}$ [see *Vasko et al.*, 2015]. In the self-consistent system this energy should be transferred to waves and can be spent for acceleration of trapped particles. Thus, for calculation of the nonlinear evolution of the amplitude of KAWs one should estimate both nonlinear currents

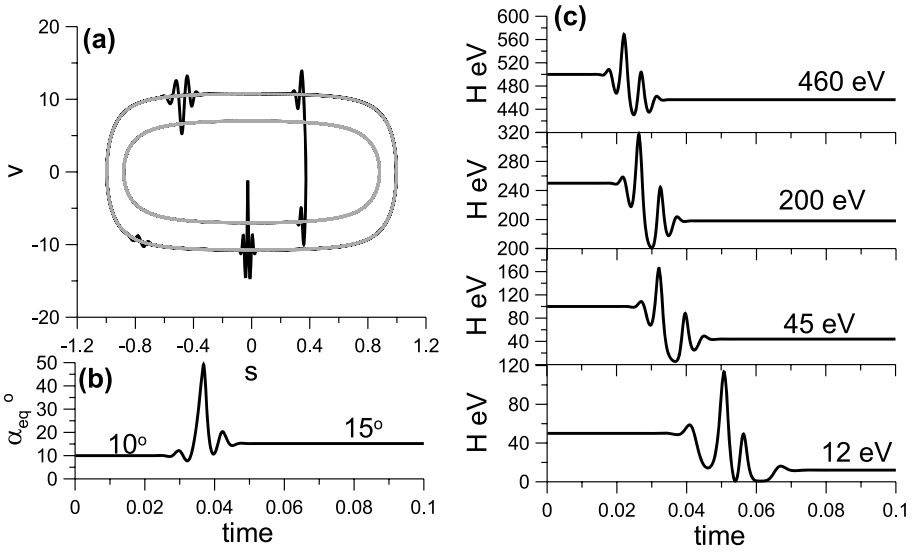

Figure 7. (a and b) An example of charged particle trajectory and the corresponding jump of the equatorial pitch angle. Grey fragments of the trajectory show particle bounce oscillations before and after interaction with KAW. (c) Several examples of jump of particle energy for different values of initial energy.

of trapped and transient electrons (see the similar estimates for whistler waves in *Shklyar and Matsumoto* [2009], *Demekhov* [2011], and *Summers et al.*[2012]). We leave this problem for further publications.

Two important properties of electron acceleration by KAWs can be considered in light of our analysis: formation of field-aligned electron population in the region of plasma injection, where most intense KAWs are observed [*Chaston et al.*, 2014; *Ergun et al.*, 2015], and effective acceleration of sub-keV electrons up to keV energies. The trapping mechanism we have discussed can potentially explain the formation of electron beams (or at least, streams with almost absent gradient of the parallel velocity distribution function) with peak parallel velocity ~(5–30) $\cdot 10^3$ km/s. To demonstrate this, we numerically integrate 10^6 trajectories and plot in Figure 8 the final velocity distribution for field-aligned electrons ($\alpha_{eq} < 30°$). One can distinguish from the figure a beam-like population of accelerated electrons with average parallel velocities ~7000 km/s. The initial pitch angle distribution is uniform, while the final pitch angle distribution contains the maximum in the small pitch angle range $\alpha_{eq} < 30°$ corresponding to the accelerated electron population. This population is generated by a combination of particle reflection from the potential wall of KAWs (see description of this mechanism of acceleration in *Bryant et al.* [1991], *Kletzing* [1994], and *Vasko et al.* [2015]), and electron trapping and acceleration by KAWs. For L shell ~6–9 the equatorial phase velocity of low band parallel chorus waves is about ~5000–10,000 km/s [e.g., *Kennel and Petschek*, 1966]. Thus, the accelerated field-aligned beam should be very unstable relative to the generation of whistler waves. This regime of generation is similar to triggered whistler wave emission [e.g., *Nunn*, 1974; *Trakhtengerts et al.*, 2003]. Therefore, we suggest that particle trapping can produce high-amplitude KAW-shape electron beams with substantial source of free energy, while secondary instability of such beams can result in efficient generation of whistler waves in the region of plasma injection. This scenario is generally confirmed by statistically higher amplitudes of whistler waves observed in the nightside inner magnetosphere [*Meredith et al.*, 2001; *Agapitov et al.*, 2013].

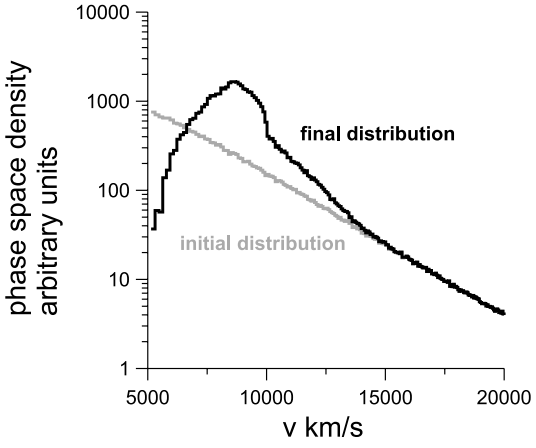

Figure 8. Velocity distributions of field-aligned electrons ($\alpha_{eq} < 30°$). Initial distribution is shown by grey color, while the final (after interaction with KAW) distribution is shown by black color.

Although we demonstrate the rapid acceleration of sub-keV electrons up to several keVs and transport of these electrons to small pitch angle range, we should admit that the proposed model cannot alone describe the formation of electron population precipitating into atmosphere and corresponding to diffusive aurora. Indeed, final energies of accelerated particles are exactly in the range aurora electron energies, but their pitch angles being rather small are still quite far from the loss cone. Thus, the proposed mechanism of electron acceleration can be responsible for formation of aurora electron (small pitch angles and keV energies) population, which should be further transported to loss cone by some high-latitude mechanisms. Alternatively, electrons accelerated by KAW can be further scattered into the loss cone by chorus waves [*Thorne et al.*, 2010; *Ni et al.*, 2014] or electron cyclotron waves [*Ni et al.*, 2011a; *Zhang et al.*, 2014].

4. Conclusions

We have considered a nonlinear mechanism of sub-keV electron acceleration by high-amplitude KAWs propagating away from the equatorial region. Our main results can be summarized as follows:

1. The parallel electric field of KAWs and the mirror force acting on electrons in an inhomogeneous magnetic field form an effective potential well for electron trapping and acceleration along magnetic field lines.
2. Trapped electrons can be transported by KAWs up to high latitudes ($\lambda \sim 40°$) with a corresponding energy gain up to several keV.
3. Acceleration of trapped electrons corresponds to a rapid decrease of the electron equatorial pitch angle: almost equatorial electrons with $\alpha_{eq} \sim 80°$ become field aligned with $\alpha_{eq} < 30°$ during a single trapping event.
4. Large amplitude of wave electrostatic potential significantly expands the range of electron velocity resonantly interacting with KAWs: even electrons with ~500 eV can be trapped and accelerated.

Appendix A: Model Description

To model kinetic Alfven wave propagating away from the equatorial plane, we use the dispersion relation provided by *Hasegawa* [1976]:

$$\omega = k_{\|} v_A \sqrt{1 + k_{\perp}^2 \rho_s^2 \left(1 + T_i/T_e\right)} \tag{A1}$$

where $v_A = B(\lambda)/\sqrt{4\pi n_e(\lambda) m_i}$ is an Alfven velocity, $\rho_s = \sqrt{2T_e m_i} c/eB(\lambda)$ is an ion acoustic scale, and $k_{\|}$ and $k_{\perp}$ are components of wave vector. Dispersion relation (A1) was derived for plasma beta (ratio of plasma and magnetic field pressures) larger than the electron to ion mass ratio. For $L = 6.6$ (geostationary orbit) the conservative estimate of the plasma beta gives ~0.1–0.2 (for hot proton density ~1–2 cm^{-3} and hot proton temperature ~1–10 keV, see *Denton et al.* [2005]). Thus, equation (A1) can be applied to describe KAW dispersion at $L > 6.6$ (the equatorial plasma beta generally increases with L).

Due to absence of a reliable information about ion and electron temperature variation along magnetic field lines, throughout the paper we consider the constant ion and electron temperatures $T_e = 100$ eV and $T_i = 1000$ eV. This approximation corresponds to the assumption of particle temperature isotropy and Maxwell distributions [see, e.g., *Whipple et al.*, 1991]. The wave frequency is $\omega = 2\pi/2$s. To model variations of the magnetic field $B(\lambda)$ and electron density $n(\lambda)$ with the magnetic latitude λ, we use the dipole model and *Denton et al.* [2006] model with $n_e = n_{eq} \cos^{-5}(\lambda)$, while the equatorial value of n_{eq} is provided by *Sheeley et al.* [2001]. We introduce the equatorial perpendicular wave number $\lambda_{\perp}$ and use the approximation $k_{\perp} = (2\pi/\lambda_{\perp})\sqrt{B(\lambda)/B_{eq}}$ [see *Watt and Rankin*, 2012, and references therein]. Thus, equation (A1) can be rewritten as $k_{\|} = (R_0\omega/v_{A,eq})K(\lambda)$ where

$$K(\lambda) = \frac{1}{b(\lambda)} \sqrt{\frac{n_e(\lambda)}{n_{eq}}} \left(1 + \frac{\kappa^2}{b(\lambda)}\right)^{-1/2} \tag{A2}$$

$b(\lambda) = B(\lambda)/B_{eq}$, $v_{A,eq}$ is an equatorial value of Alfven velocity, $R_0 = R_E L$ is a scale of magnetic field inhomogeneity, and $\kappa = 2\pi\sqrt{2T_e m_i} c\sqrt{1 + T_i/T_e}/\lambda_{\perp} eB_{eq}$. We also use dimensionless parameter $\chi = R_0\omega/v_{A,eq} \approx 250(2\text{s}/T)(L/9)^2$ and $T = 2$ s is a wave period.

In the kinetic Alfven wave the approximate relation between parallel component of the vector potential $A_\parallel$ and scalar potential φ can be written in following form [see, e.g., *Watt and Rankin*, 2010]:

$$\frac{\partial A_\parallel}{\partial z} = -\frac{c}{v_A^2}\frac{\partial \varphi}{\partial t} \tag{A3}$$

where $z = R_0 \int \sqrt{1+3\sin^2\lambda}\cos\lambda d\lambda$ is a field-aligned coordinate. Assuming that φ and $A_\parallel$ depend on phase $\psi = \int^z k_\parallel dz - \omega t$, we solve equation (A3): $A_\parallel = c\omega\varphi/k_\parallel v_A^2$. Thus, the total parallel electric field can be written as

$$E_\parallel = -\frac{\partial \varphi}{\partial z} - \frac{1}{c}\frac{\partial A_\parallel}{\partial t} = -k_\parallel\left(1-\frac{\omega^2}{k_\parallel^2 v_A^2}\right)\varphi = k_\parallel k_\perp^2 \rho_s^2\left(1+T_i/T_e\right)\varphi \tag{A4}$$

We introduce the generalized potential $\Phi = -\Phi_0 w(z) f(\psi)$ and write $E_\parallel = -k_\parallel \Phi = -\partial\Phi/\partial z$ with

$$w(z) = g(z)k_\perp^2\rho_s^2\left(1+T_i/T_e\right) = \kappa^2 g(z)/b(z) \tag{A5}$$

where function $g(z)$ defines the growth of the scalar potential from zero value up to an amplitude Φ_0. We use $g(z)$ corresponding to the monotonical increase of Φ within 5° near the equatorial plane. For $|\lambda| > 5°$ function g is equal to 1.

Acknowledgments
R. Rankin acknowledges financial support from NSERC, the National Engineering and Research Council of Canada, and the Canadian Space Agency. A. Artemyev is grateful to Dmitry Zimin Dynasty Foundation for their support. All the new data used in this paper are obtained from analytical formulas provided here. Corresponding parameters are listed in the text.

References

Agapitov, O., A. Artemyev, V. Krasnoselskikh, Y. V. Khotyaintsev, D. Mourenas, H. Breuillard, M. Balikhin, and G. Rolland (2013), Statistics of whistler mode waves in the outer radiation belt: Cluster STAFF-SA measurements, *J. Geophys. Res. Space Physics*, *118*, 3407–3420, doi:10.1002/jgra.50312.

Akasofu, S.-I. (1974), A study of auroral displays photographed from the DMSP-2 satellite and from the Alaska meridian chain of stations, *Space Sci. Rev.*, *16*, 617–725, doi:10.1007/BF00182598.

Angelopoulos, V., J. A. Chapman, F. S. Mozer, J. D. Scudder, C. T. Russell, K. Tsuruda, T. Mukai, T. J. Hughes, and K. Yumoto (2002), Plasma sheet electromagnetic power generation and its dissipation along auroral field lines, *J. Geophys. Res.*, *107*, 1181, doi:10.1029/2001JA900136.

Arnold, V. I., V. V. Kozlov, and A. I. Neishtadt (2006), *Mathematical Aspects of Classical and Celestial Mechanics, Dynamical Systems III. Encyclopedia of Mathematical Sciences*, 3rd ed., Springer, New York.

Arnoldy, R. L. (1974), Auroral particle precipitation and Birkeland currents, *Rev. Geophys.*, *12*, 217–231, doi:10.1029/RG012i002p00217.

Artemyev, A., V. Krasnoselskikh, O. Agapitov, D. Mourenas, and G. Rolland (2012), Non-diffusive resonant acceleration of electrons in the radiation belts, *Phys. Plasmas*, *19*, 122901, doi:10.1063/1.4769726.

Artemyev, A. V., A. I. Neishtadt, L. M. Zelenyi, and D. L. Vainchtein (2010), Adiabatic description of capture into resonance and surfatron acceleration of charged particles by electromagnetic waves, *Chaos*, *20*(4), 43128, doi:10.1063/1.3518360.

Artemyev, A. V., A. A. Vasiliev, D. Mourenas, O. Agapitov, and V. Krasnoselskikh (2013), Nonlinear electron acceleration by oblique whistler waves: Landau resonance vs. Cyclotron resonance, *Phys. Plasmas*, *20*, 122901, doi:10.1063/1.4836595.

Artemyev, A. V., O. Agapitov, F. Mozer, and V. Krasnoselskikh (2014), Thermal electron acceleration by localized bursts of electric field in the radiation belts, *Geophys. Res. Lett.*, *41*, 5734–5739, doi:10.1002/2014GL061248.

Artemyev, A. V., O. V. Agapitov, D. Mourenas, V. V. Krasnoselskikh, and F. S. Mozer (2015), Wave energy budget analysis in the Earth's radiation belts uncovers a missing energy, *Nat. Commun.*, *6*, 8143, doi:10.1038/ncomms8143.

Balikhin, M., M. Gedalin, and A. Petrukovich (1993), New mechanism for electron heating in shocks, *Phys. Rev. Lett.*, *70*, 1259–1262, doi:10.1103/PhysRevLett.70.1259.

Bell, T. F. (1984), The nonlinear gyroresonance interaction between energetic electrons and coherent VLF waves propagating at an arbitrary angle with respect to the Earth's magnetic field, *J. Geophys. Res.*, *89*, 905–918, doi:10.1029/JA089iA02p00905.

Bryant, D. A., A. C. Cook, Z.-S. Wang, U. de Angelis, and C. H. Perry (1991), Turbulent acceleration of auroral electrons, *J. Geophys. Res.*, *96*, 13,829–13,839, doi:10.1029/91JA01105.

Chaston, C. C., C. W. Carlson, R. E. Ergun, and J. P. McFadden (2000), Alfvén waves, density cavities and electron acceleration observed from the FAST spacecraft, *Phys. Scr.*, *T84*, 64–68, doi:10.1238/Physica.Topical.084a00064.

Chaston, C. C., J. W. Bonnell, L. M. Peticolas, C. W. Carlson, J. P. McFadden, and R. E. Ergun (2002), Driven Alfven waves and electron acceleration: A FAST case study, *Geophys. Res. Lett.*, *29*, doi:10.1029/2001GL013842.

Chaston, C. C., C. Salem, J. W. Bonnell, C. W. Carlson, R. E. Ergun, R. J. Strangeway, and J. P. McFadden (2008), The turbulent Alfvénic aurora, *Phys. Rev. Lett.*, *100*(17), 175003, doi:10.1103/PhysRevLett.100.175003.

Chaston, C. C., J. W. Bonnell, L. Clausen, and V. Angelopoulos (2012), Energy transport by kinetic-scale electromagnetic waves in fast plasma sheet flows, *J. Geophys. Res.*, *117*, A09202, doi:10.1029/2012JA017863.

Chaston, C. C., J. W. Bonnell, and C. Salem (2014), Heating of the plasma sheet by broadband electromagnetic waves, *Geophys. Res. Lett.*, *41*, 8185–8192, doi:10.1002/2014GL062116.

Damiano, P. A., and A. N. Wright (2005), Two-dimensional hybrid MHD-kinetic electron simulations of an Alfvén wave pulse, *J. Geophys. Res.*, *110*, A01201, doi:10.1029/2004JA010603.

Demekhov, A. G. (2011), Generation of VLF emissions with the increasing and decreasing frequency in the magnetosperic cyclotron maser in the backward wave oscillator regime, *Radiophys. Quantum Electron.*, *53*, 609–622, doi:10.1007/s11141-011-9256-x.

Denton, M. H., M. F. Thomsen, H. Korth, S. Lynch, J. C. Zhang, and M. W. Liemohn (2005), Bulk plasma properties at geosynchronous orbit, *J. Geophys. Res.*, *110*, A07223, doi:10.1029/2004JA010861.

Denton, R. E., K. Takahashi, I. A. Galkin, P. A. Nsumei, X. Huang, B. W. Reinisch, R. R. Anderson, M. K. Sleeper, and W. J. Hughes (2006), Distribution of density along magnetospheric field lines, *J. Geophys. Res.*, *111*, A04213, doi:10.1029/2005JA011414.

Ergun, R. E., K. A. Goodrich, J. E. Stawarz, L. Andersson, and V. Angelopoulos (2015), Large-amplitude electric fields associated with bursty bulk flow braking in the Earth's plasma sheet, *J. Geophys. Res.*, *120*, 1832–1844, doi:10.1002/2014JA020165.
Fu, X., et al. (2014), Whistler anisotropy instabilities as the source of banded chorus: Van Allen probes observations and particle-in-cell simulations, *J. Geophys. Res.*, *119*, 8288–8298, doi:10.1002/2014JA020364.
Gabrielse, C., V. Angelopoulos, A. Runov, and D. L. Turner (2012), The effects of transient, localized electric fields on equatorial electron acceleration and transport toward the inner magnetosphere, *J. Geophys. Res.*, *117*, A10213, doi:10.1029/2012JA017873.
Ganushkina, N. Y., O. A. Amariutei, Y. Y. Shprits, and M. W. Liemohn (2013), Transport of the plasma sheet electrons to the geostationary distances, *J. Geophys. Res.*, *118*, 82–98, doi:10.1029/2012JA017923.
Génot, V., P. Louarn, and F. Mottez (2004), Alfvén wave interaction with inhomogeneous plasmas: Acceleration and energy cascade towards small-scales, *Ann. Geophys.*, *22*, 2081–2096, doi:10.5194/angeo-22-2081-2004.
Hasegawa, A. (1976), Particle acceleration by MHD surface wave and formation of aurora, *J. Geophys. Res.*, *81*, 5083–5090, doi:10.1029/JA081i028p05083.
Hasegawa, A., and K. Mima (1976), Exact solitary Alfvén wave, *Phys. Rev. Lett.*, *37*, 690–693, doi:10.1103/PhysRevLett.37.690.
Hasegawa, A., and K. Mima (1978), Anomalous transport produced by kinetic Alfven wave turbulence, *J. Geophys. Res.*, *83*, 1117–1123, doi:10.1029/JA083iA03p01117.
Horne, R. B., G. V. Wheeler, and H. S. C. K. Alleyne (2000), Proton and electron heating by radially propagating fast magnetosonic waves, *J. Geophys. Res.*, *105*, 27,597–27,610, doi:10.1029/2000JA000018.
Karney, C. F. F. (1978), Stochastic ion heating by a lower hybrid wave, *Phys. Fluids*, *21*, 1584–1599, doi:10.1063/1.862406.
Karpman, V. I., and D. R. Shklyar (1972), Nonlinear damping of potential monochromatic waves in an inhomogeneous plasma, *Sov. Phys. J. Exper. Theor. Phys.*, *35*, 500.
Karpman, V. I., J. N. Istomin, and D. R. Shklyar (1974), Nonlinear theory of a quasi-monochromatic whistler mode packet in inhomogeneous plasma, *Plasma Phys.*, *16*, 685–703, doi:10.1088/0032-1028/16/8/001.
Kennel, C. F., and H. E. Petschek (1966), Limit on stably trapped particle fluxes, *J. Geophys. Res.*, *71*, 1–28.
Kletzing, C. A. (1994), Electron acceleration by kinetic Alfvén waves, *J. Geophys. Res.*, *99*, 11,095–11,104, doi:10.1029/94JA00345.
Kletzing, C. A., J. D. Scudder, E. E. Dors, and C. Curto (2003), Auroral source region: Plasma properties of the high-latitude plasma sheet, *J. Geophys. Res.*, *108*, 1360, doi:10.1029/2002JA009678.
Laval, G., and R. Pellat (1970), Particle acceleration by electrostatic waves propagating in an inhomogeneous plasma, *J. Geophys. Res.*, *75*, 3255–3256, doi:10.1029/JA075i016p03255.
Li, W., R. M. Thorne, J. Bortnik, Y. Nishimura, V. Angelopoulos, L. Chen, J. P. McFadden, and J. W. Bonnell (2010), Global distributions of suprathermal electrons observed on THEMIS and potential mechanisms for access into the plasmasphere, *J. Geophys. Res.*, *115*, A00J10, doi:10.1029/2010JA015687.
Lysak, R. L., and Y. Song (2003), Kinetic theory of the Alfvén wave acceleration of auroral electrons, *J. Geophys. Res.*, *108*, 8005, doi:10.1029/2002JA009406.
Malaspina, D. M., J. R. Wygant, R. E. Ergun, G. D. Reeves, R. M. Skoug, and B. A. Larsen (2015), Electric field structures and waves at plasma boundaries in the inner magnetosphere, *J. Geophys. Res. Space Physics*, *120*, 4246–4263, doi:10.1002/2015JA021137.
Meredith, N. P., R. B. Horne, and R. R. Anderson (2001), Substorm dependence of chorus amplitudes: Implications for the acceleration of electrons to relativistic energies, *J. Geophys. Res.*, *178*(13), 165–13, doi:10.1029/2000JA900156.
Mottez, F., and V. Génot (2011), Electron acceleration by an Alfvénic pulse propagating in an auroral plasma cavity, *J. Geophys. Res.*, *116*, A00K15, doi:10.1029/2010JA016367.
Mourenas, D., A. V. Artemyev, O. V. Agapitov, V. Krasnoselskikh, and F. S. Mozer (2015), Very oblique whistler generation by low-energy electron streams, *J. Geophys. Res.*, *120*, 3665–3683, doi:10.1002/2015JA021135.
Mozer, F. S., S. D. Bale, J. W. Bonnell, C. C. Chaston, I. Roth, and J. Wygant (2013), Megavolt parallel potentials arising from double-layer streams in the Earth's outer radiation belt, *Phys. Rev. Lett.*, *111*(23), 235002, doi:10.1103/PhysRevLett.111.235002.
Mozer, F. S., O. Agapitov, V. Krasnoselskikh, S. Lejosne, G. D. Reeves, and I. Roth (2014), Direct observation of radiation-belt electron acceleration from electron-volt energies to megavolts by nonlinear whistlers, *Phys. Rev. Lett.*, *113*(3), 35001, doi:10.1103/PhysRevLett.113.035001.
Mozer, F. S., O. Agapitov, A. Artemyev, J. F. Drake, V. Krasnoselskikh, S. Lejosne, and I. Vasko (2015), Time domain structures: What and where they are, what they do, and how they are made, *Geophys. Res. Lett.*, *42*, 3627–3638, doi:10.1002/2015GL063946.
Neishtadt, A. I. (1999), *Hamiltonian Systems With Three or More Degrees of Freedom*, NATO ASI Series C, vol. 533, Kluwer Acad. Publ., Dordrecht, Netherlands.
Neishtadt, A. I. (2014), Averaging, passage through resonances, and capture into resonance in two-frequency systems, *Russ. Math. Surv.*, *69*(5), 771–843.
Ni, B., R. M. Thorne, R. B. Horne, N. P. Meredith, Y. Y. Shprits, L. Chen, and W. Li (2011a), Resonant scattering of plasma sheet electrons leading to diffuse auroral precipitation: 1. Evaluation for electrostatic electron cyclotron harmonic waves, *J. Geophys. Res.*, *116*, A04218, doi:10.1029/2010JA016232.
Ni, B., R. M. Thorne, N. P. Meredith, R. B. Horne, and Y. Y. Shprits (2011b), Resonant scattering of plasma sheet electrons leading to diffuse auroral precipitation: 2. Evaluation for whistler mode chorus waves, *J. Geophys. Res.*, *116*, A04219, doi:10.1029/2010JA016233.
Ni, B., J. Liang, R. M. Thorne, V. Angelopoulos, R. B. Horne, M. Kubyshkina, E. Spanswick, E. F. Donovan, and D. Lummerzheim (2012), Efficient diffuse auroral electron scattering by electrostatic electron cyclotron harmonic waves in the outer magnetosphere: A detailed case study, *J. Geophys. Res.*, *117*, A01218, doi:10.1029/2011JA017095.
Ni, B., J. Bortnik, Y. Nishimura, R. M. Thorne, W. Li, V. Angelopoulos, Y. Ebihara, and A. T. Weatherwax (2014), Chorus wave scattering responsible for the Earth's dayside diffuse auroral precipitation: A detailed case study, *J. Geophys. Res. Space Physics*, *119*, 897–908, doi:10.1002/2013JA019507.
Northrop, T. G. (1963), *The Adiabatic Motion of Charged Particles*, John Wiley, New York, London, and Sydney.
Nunn, D. (1971), Wave-particle interactions in electrostatic waves in an inhomogeneous medium, *J. Plasma Phys.*, *6*, 291–307, doi:10.1017/S0022377800006061.
Nunn, D. (1974), A self-consistent theory of triggered VLF emissions, *Plan. Space Sci.*, *22*, 349–378, doi:10.1016/0032-0633(74)90070-1.
Potapenko, I. F., C. A. de Azevedo, and P. H. Sakanaka (2000), Electron heating and acceleration by Alfvén waves with varying phase velocity, *Phys. Scr.*, *62*, 486–490, doi:10.1238/Physica.Regular.062a00486.
Schulz, M., and L. J. Lanzerotti (1974), *Particle Diffusion in the Radiation Belts*, Springer, New York.
Sheeley, B. W., M. B. Moldwin, H. K. Rassoul, and R. R. Anderson (2001), An empirical plasmasphere and trough density model: CRRES observations, *J. Geophys. Res.*, *106*, 25,631–25,642, doi:10.1029/2000JA000286.
Shklyar, D., and H. Matsumoto (2009), Oblique whistler-mode waves in the inhomogeneous magnetospheric plasma: Resonant interactions with energetic charged particles, *Surv. Geophys.*, *30*, 55–104, doi:10.1007/s10712-009-9061-7.

Shklyar, D. R. (1981), Stochastic motion of relativistic particles in the field of a monochromatic wave, *Sov. Phys. J. Exper. Theor. Phys.*, *53*, 1197–1192.

Shklyar, D. R. (2011), On the nature of particle energization via resonant wave-particle interaction in the inhomogeneous magnetospheric plasma, *Ann. Geophys.*, *29*, 1179–1188, doi:10.5194/angeo-29-1179-2011.

Sitnov, M. I., N. A. Tsyganenko, A. Y. Ukhorskiy, and P. C. Brandt (2008), Dynamical data-based modeling of the storm-time geomagnetic field with enhanced spatial resolution, *J. Geophys. Res.*, *113*, A07218, doi:10.1029/2007JA013003.

Summers, D., Y. Omura, Y. Miyashita, and D.-H. Lee (2012), Nonlinear spatiotemporal evolution of whistler mode chorus waves in Earth's inner magnetosphere, *J. Geophys. Res.*, *117*, A09206, doi:10.1029/2012JA017842.

Thorne, R. M., B. Ni, X. Tao, R. B. Horne, and N. P. Meredith (2010), Scattering by chorus waves as the dominant cause of diffuse auroral precipitation, *Nature*, *467*, 943–946, doi:10.1038/nature09467.

Tikhonchuk, V. T., and R. Rankin (2002), Parallel potential driven by a kinetic Alfvén wave on geomagnetic field lines, *J. Geophys. Res.*, *107*, 1104, doi:10.1029/2001JA000231.

Trakhtengerts, V. Y., A. G. Demekhov, Y. Hobara, and M. Hayakawa (2003), Phase-bunching effects in triggered VLF emissions: Antenna effect, *J. Geophys. Res.*, *108*, 1160, doi:10.1029/2002JA009415.

Tsyganenko, N. A., H. J. Singer, and J. C. Kasper (2003), Storm-time distortion of the inner magnetosphere: How severe can it get?, *J. Geophys. Res.*, *108*, 1209, doi:10.1029/2002JA009808.

Vasko, I. Y., O. V. Agapitov, F. Mozer, and A. V. Artemyev (2015), Thermal electron acceleration by electric field spikes in the outer radiation belt: Generation of field-aligned pitch angle distributions, *J. Geophys. Res. Space Physics*, *120*, 8616–8632, doi:10.1002/2015JA021644.

Watt, C. E. J., and R. Rankin (2009), Electron trapping in shear Alfvén waves that power the aurora, *Phys. Rev. Lett.*, *102*(4), 45002, doi:10.1103/PhysRevLett.102.045002.

Watt, C. E. J., and R. Rankin (2010), Do magnetospheric shear Alfvén waves generate sufficient electron energy flux to power the aurora?, *J. Geophys. Res.*, *115*, A07224, doi:10.1029/2009JA015185.

Watt, C. E. J., and R. Rankin (2012), Alfvén wave acceleration of auroral electrons in warm magnetospheric plasma, in *Auroral Phenomenology and Magnetospheric Processes: Earth and Other Planets, Geophys. Monogr. Ser.*, vol. 197, pp. 251–260, AGU, Washington, D. C., doi:10.1029/2011GM001171

Watt, C. E. J., R. Rankin, and R. Marchand (2004), Kinetic simulations of electron response to shear Alfvén waves in magnetospheric plasmas, *Phys. Plasmas*, *11*, 1277–1284, doi:10.1063/1.1647140.

Watt, C. E. J., R. Rankin, I. J. Rae, and D. M. Wright (2005), Self-consistent electron acceleration due to inertial Alfvén wave pulses, *J. Geophys. Res.*, *110*, A10S07, doi:10.1029/2004JA010877.

Watt, C. E. J., R. Rankin, I. J. Rae, and D. M. Wright (2006), Inertial Alfvén waves and acceleration of electrons in nonuniform magnetic fields, *Geophys. Res. Lett.*, *33*, L02106, doi:10.1029/2005GL024779.

Whipple, E., R. Puetter, and M. Rosenberg (1991), A two-dimensional, time-dependent, near-earth magnetotail, *Adv. Space Res.*, *11*, 133–142, doi:10.1016/0273-1177(91)90024-E.

Wygant, J. R., et al. (2002), Evidence for kinetic Alfvén waves and parallel electron energization at 4–6 R_E altitudes in the plasma sheet boundary layer, *J. Geophys. Res.*, *107*, 1201, doi:10.1029/2001JA900113.

Zhang, X., V. Angelopoulos, B. Ni, R. M. Thorne, and R. B. Horne (2014), Extent of ECH wave emissions in the Earth's magnetotail, *J. Geophys. Res. Space Physics*, *119*, 5561–5574, doi:10.1002/2014JA019931.